AGU PUBLICATIONS

JGR

Journal of Geophysical Research: Oceans

RESEARCH ARTICLE

10.1002/2014JC010094

Special Section:
Early scientific results from the salinity measuring satellites Aquarius/SAC-D and SMOS

Evaluation of sea-surface salinity observed by Aquarius

Hiroto Abe[1] and Naoto Ebuchi[1]

[1]Institute of Low Temperature Science, Hokkaido University, Sapporo, Japan

Abstract Sea-surface salinity (SSS) observed by Aquarius was compared with global observations from Argo floats and offshore moored buoys to evaluate the quality of satellite SSS data and to assess error structures. Aquarius products retrieved by different algorithms (Aquarius Official Release version 3.0 [V3.0], Combined Active-Passive [CAP] algorithm version 3.0, and Remote Sensing Systems test bed algorithm version 3) were compared. The Aquarius SSS was in good agreement with in situ salinity measurements for all three products. Root-mean-square (rms) differences of the salinity residual, with respect to Argo salinity, ranged from 0.41 to 0.52 psu. These three Aquarius products exhibit high SSS deviation from Argo salinity under lower sea-surface temperature conditions ($<10^{\circ}$C) due to lower sensitivity of microwave emissivity to SSS. The CAP product deviates under strong wind conditions (>10 m s^{-1}), probably due to model bias and uncertainty associated with sea-surface roughness. Furthermore, significant SSS differences between ascending (south-to-north) and descending (north-to-south) paths were detected. The monthly averaged Aquarius SSS ($1^{\circ} \times 1^{\circ}$ grid) was also compared with outputs from the ocean data optimal interpolation (OI) system operated by the Japan Agency for Marine-Earth Science Technology (JAMSTEC) and the ocean data assimilation system used by the Meteorological Research Institute, Japan Meteorological Agency (MRI/JMA). Negative bias, attributed to near-surface salinity stratification by precipitation, was detected in tropical regions. For 40°S–40°N, rms difference, with respect to JAMSTEC OI, is 0.27 psu for the V3.0, while the CAP product rms difference is only 0.22 psu, which is close to the Aquarius mission goal.

Key Points:
- Sea-surface salinity (SSS) observed by Aquarius was evaluated using in situ data
- SSS retrieved by three different algorithms were compared with each other
- Error structure of the retrieved SSS was characterized by residual analyses

Correspondence to:
H. Abe,
abe@lowtem.hokudai.ac.jp

Citation:
Abe, H., and N. Ebuchi (2014), Evaluation of sea-surface salinity observed by Aquarius, *J. Geophys. Res. Oceans*, *119*, 8109–8121, doi:10.1002/2014JC010094.

Received 30 APR 2014
Accepted 27 OCT 2014
Accepted article online 31 OCT 2014
Published online 28 NOV 2014

1. Introduction

Aquarius is an instrument for observing the sea-surface salinity (SSS) of the global oceans. It was developed by the National Aeronautics and Space Administration (NASA) and was installed on the SAC-D spacecraft, launched on 10 June 2011 and operated by Argentina's Comisión Nacional de Actividades Espaciales (CONAE). The Aquarius is a combination of a radiometer and a scatterometer operating in the L-band. The radiometer measures microwave radiation emitted from the sea surface at a frequency of 1.413 GHz, where the emissivity is relatively sensitive to SSS [*Swift and McIntosh*, 1983; *Lagerloef et al*., 2008]. The scatterometer operating at 1.260 GHz provides coincident sea-surface roughness information, which is a critical correction term for retrieving SSS [*LeVine et al*., 2010].

The goal of the Aquarius mission is to globally measure monthly mean SSS with an accuracy of 0.2 psu over a spatial smoothing scale of 150 km. Because Aquarius does not measure SSS directly but measures the electromagnetic radiation signal emitted from the sea surface, validations of the retrieved SSS are necessary to evaluate the quality of the data and to assess the error structures. In the present study, Aquarius along-track SSS observations were compared with in situ salinity measurements from Argo floats and offshore moored buoys. In addition, the monthly averaged Aquarius SSS was compared with results from the ocean data optimal interpolation system operated by the Japan Agency for Marine-Earth Science and Technology (JAMSTEC) and the ocean data assimilation system used by the Meteorological Research Institute, Japan Meteorological Agency (MRI/JMA). Residual analyses were conducted to clarify the error structures. Evaluation results obtained from the different Aquarius products are compared with each other and possible causes of errors are discussed in terms of the measurement principles employed by the Aquarius mission and differences in the SSS retrieval algorithms. The paper is organized as follows: section 2 describes the data used, sections 3 and 4 describe the results obtained from analyses of along-track and monthly averaged SSS, respectively, and section 5 presents a brief summary.

2. Data

2.1. Aquarius SSS Products

2.1.1. Level 2 Products

In this study, we used three versions of the Aquarius Level 2 along-track SSS: the Aquarius Official Release SSS product version 3.0 [*NASA JPL PO.DAAC*, 2014; *Patt*, 2014], the SSS product produced by the Combined Active-Passive (CAP) algorithm version 3.0 [*Yueh and Chaubell*, 2012], and the Remote Sensing Systems SSS test bed product version 3 [*Wentz and LeVine*, 2012; *Meissner*, 2013]. Level 2 along-track data were compared with in situ salinity observed by Argo floats and moored buoys.

The Aquarius Official Release SSS product version 3.0 [*NASA JPL PO.DAAC*, 2014; *Patt*, 2014], hereafter referred to as V3.0, produced by the NASA Jet Propulsion Laboratory (JPL), is the latest version of the SSS product produced by the Aquarius project and can be downloaded from the Physical Oceanography Distributed Active Archive Center (PO.DAAC) FTP site. The V3.0 SSS data for September 2011 to October 2013 were analyzed. The V3.0 algorithm utilizes the radar cross section measured by Aquarius scatterometer for sea-surface roughness correction. To correct the ascending-descending bias, discussed in section 3.2, monthly averaged SSS fields from the Hybrid Coordinate Ocean Model (HYCOM) [*Chassignet et al.*, 2009] ocean data assimilation system, a real-time 1/12° global ocean nowcast/forecast model developed and operated by the United States Navy, are employed in the V3.0 algorithm.

An independently developed algorithm known as the Combined Active-Passive (CAP) algorithm [*Yueh and Chaubell*, 2012] is also used to retrieve SSS from the brightness temperature and the radar cross section measured by Aquarius. The algorithm computes the SSS by minimizing the least squares error between measurements and model functions of brightness temperatures and radar backscatter. The CAP algorithm does not correct for the ascending-descending bias using HYCOM SSS fields, as is done in the V3.0 algorithm. In this study, we used CAP version 3.0 SSS product, hereafter referred to as CAP V3.0. CAP data for the same period as the V3.0 were used.

Furthermore, we analyzed the SSS product retrieved by the Remote Sensing Systems test bed version 3 algorithm, hereafter referred to as RSS [*Wentz and LeVine*, 2012; *Meissner*, 2013]. During the early stages of Aquarius algorithm refinements, the RSS test bed algorithm was incorporated into the V3.0 algorithm. Similar to the V3.0 algorithm, the RSS algorithm also uses the radar cross section measured by the Aquarius scatterometer to correct for sea-surface roughness and a correction for ascending-descending bias that employs HYCOM SSS data. The RSS data for September 2011 to May 2013 were used.

We used quality flags assigned in each of the Level 2 along-track SSS data sets to remove outliers. Consistent with *Patt* [2014], we employed the following quality flags: (1) land contamination, (2) sea ice contamination, (3) wind/foam contamination, (4) nonnominal navigation, (5) SA overflow, (6) roughness correction, (7) pointing anomaly, (8) rad Tb consistency, (9) cold water, (10) RFI level, (11) moon reflected radiation/galaxy reflected radiation, and (12) excessive ascending/descending difference (see *Patt* [2014] for more detail). Aquarius SSS data were discarded whenever any of these flags were triggered.

2.1.2. Level 3 Products

We analyzed four versions of Aquarius Level 3 monthly gridded SSS data: the Aquarius Official Release SSS product versions 1.3, 2.0, 3.0, and CAP V3.0. RSS has not released Level 3 products. Although our main target is the evaluation of the latest versions of the Aquarius SSS products (V3.0 and CAP V3.0), we also used the older versions (V1.3 and 2.0) to highlight improvements in the sensor calibration and retrieval algorithm. Level 3 Aquarius SSS is gridded using Level 2 along-track Aquarius SSS. The SSSs observed by beams 1, 2, and 3 are merged by spatial filtering to represent SSS on a $1^\circ \times 1^\circ$ grid for each month for the official products and the CAP product. Level 3 processing discards SSS data flagged as being contaminated with severe RFI, while data flagged as moderate RFI contamination are not discarded (see *Patt* [2014] for more details); therefore, Level 3 SSS fields may be affected by RFI contaminations to some extent. The Level 3 monthly gridded data for the period September 2011 to October 2013 were compared with outputs from the JAMSTEC ocean data OI system and the MRI/JMA ocean data assimilation system.

2.2. In Situ Salinity Measurements

Argo float salinity profiles were obtained from the Global Data Assembly Center website for comparison with the Aquarius SSS data. A global ocean comparison was conducted for the period September 2011 to

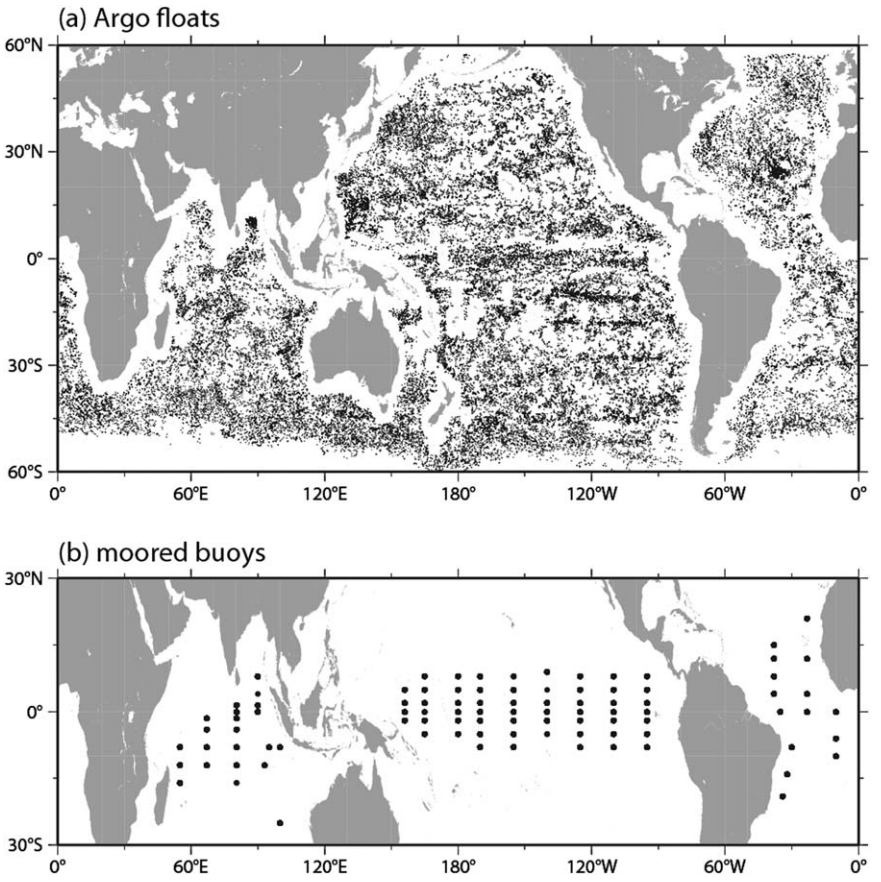

Figure 1. Locations of sea-surface salinity (SSS) measurements by (a) Argo floats and (b) moored buoys collocated with Aquarius Level 2 V3.0 SSS for beam 1. The number of Argo floats observations is 162,566 and the number of moored buoys locations and observations are 84 and 8155, respectively.

October 2013, with Argo salinity data observed at 12.5 dbar (12–13 m depth equivalence) or shallower. Additionally, temperature data in the Argo profiles were used for residual analysis.

Near-surface salinity data observed by ocean buoys moored in the tropical regions were also used for the comparison. These buoys are operated by the Tropical Atmosphere Ocean and Triangle Trans-Ocean Buoy

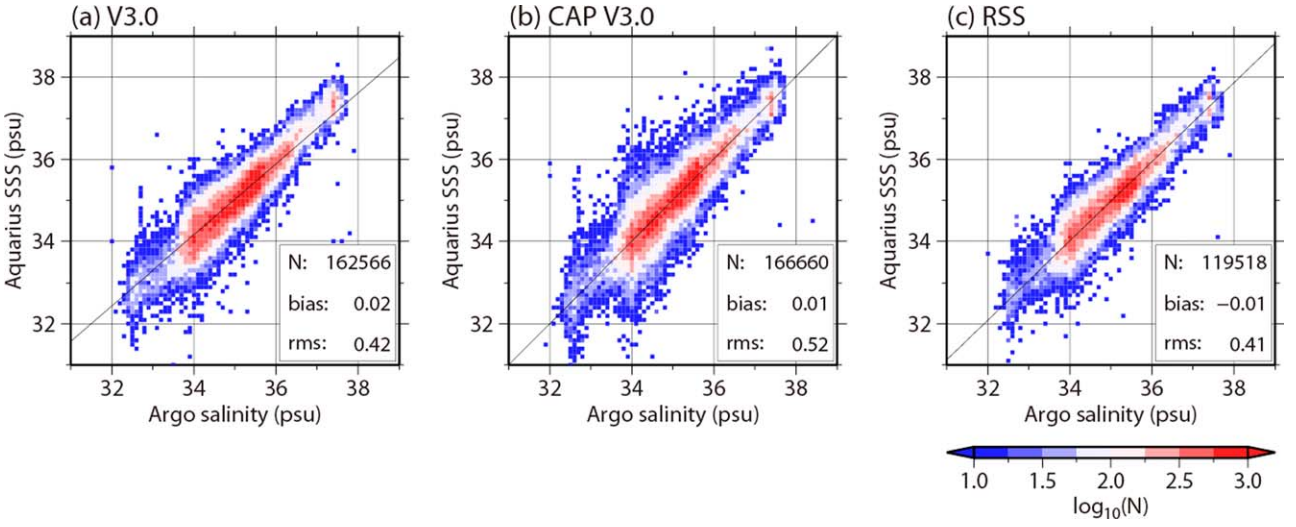

Figure 2. Comparisons of sea-surface salinity (SSS) measured by Aquarius with near-surface salinity observed by Argo floats. (a) V3.0, (b) CAP V3.0, and (c) RSS algorithms for beam 1. Numbers of the collocated data in 0.1 psu × 0.1 psu bins are shown in color.

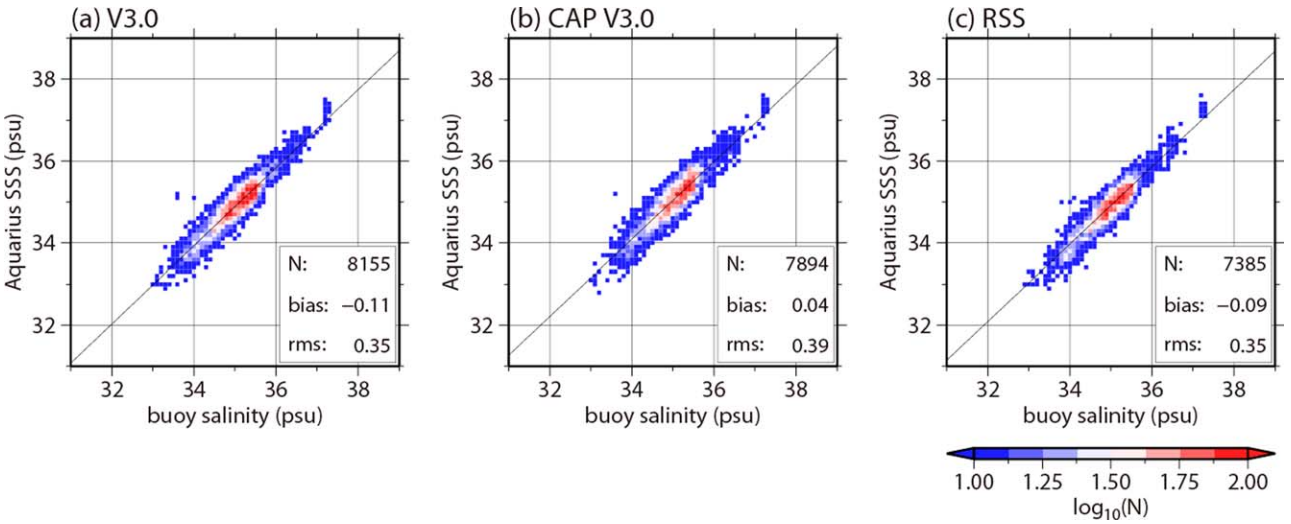

Figure 3. Same as Figure 2, except for comparisons with near-surface salinity observed by moored buoys.

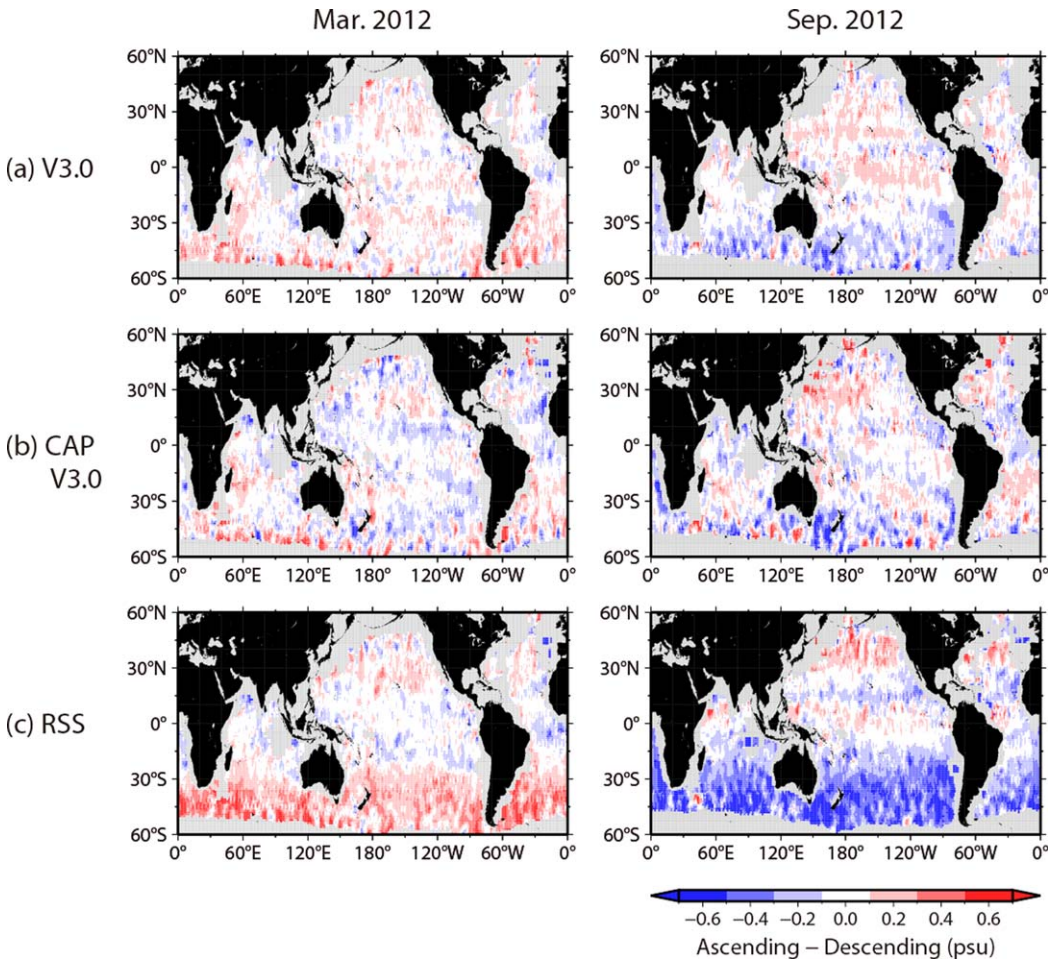

Figure 4. Aquarius Level 2 sea-surface salinity (SSS) difference between ascending and descending paths, (a) V3.0, (b) CAP V3.0, and (c) RSS beam 1 products for (left) March 2012 and (right) September 2012. Each of the 1.0° × 1.0° grids is masked by gray when no data is available.

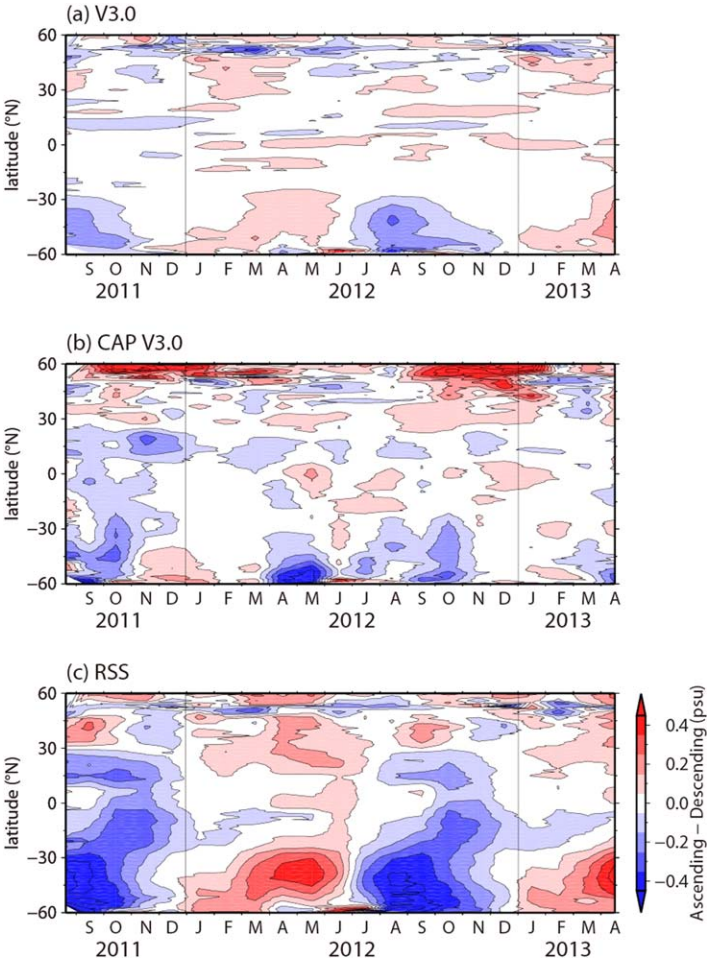

Figure 5. Latitude-time diagram of the ascending-descending difference (A/D difference) calculated using (a) V3.0, (b) CAP V3.0, and (c) RSS products for beam 1. This diagram was produced by zonally averaging the A/D difference in Figure 4.

Network (TAO/TRITON), the Pilot Research Moored Array in the Tropical Atlantic (PIRATA), and the Research Moored Array for African-Asian-Australian Monsoon Analysis and Prediction (RAMA) [*McPhaden et al.*, 1998; *Kuroda*, 2002; *Bourlès et al.*, 2008; *McPhaden et al.*, 2009]. The comparison was conducted using the daily averaged data observed at 1 m for the same period as that for the Argo data.

The Aquarius SSS data were collocated with the Argo and buoy near-surface salinity data with temporal and spatial separations of $<$12 h and 200 km, respectively (Figure 1).

2.3. Monthly Gridded SSS Fields

Aquarius Level 3 monthly averaged SSS data were compared with outputs from the JAMSTEC ocean data OI system and the MRI/JMA ocean data assimilation system.

Three-dimensional (3-D) optimally interpolated grid point values from JAMSTEC's Monthly Objective Analysis using Argo data (MOAA GPV), a global monthly temperature and salinity (T/S) gridded data set [*Hosoda et al.*, 2008], were used. These gridded values are result from an optimal interpolation (OI) method that employs in situ T/S data obtained from various hydrographic instruments, including Argo floats, TRITON buoys, and available conductivity-temperature-depth (CTD) casts. The horizontal resolution is 1.0° × 1.0° for the global oceans. The salinity data at the depth of 10 dbar (10 m depth equivalence) for September 2011 to October 2013 were employed.

In addition, we used the gridded global monthly T/S datasets from the data assimilation system developed by MRI/JMA, known as the Multivariate Ocean 3-D Variational Estimation/MRI Community Ocean Model (MOVE/MRI.COM). In situ observations of subsurface T/S obtained from ships, profiling floats, and moored and drifting buoys, as well as satellite altimeter data, are assimilated into the model [*Usui et al.*, 2006]. The horizontal resolution is 1.0° × 1.0° for the global oceans, except for the region 15°S–15°N, where latitudinal grid spacing decreases to a minimum of 0.3° for 6°S–6°N. Model values were regridded from this irregular grid into a regular 1° × 1° grid using simple bin-averaging. The salinity data at 1 m depth for September 2011 to December 2012 were used.

3. Evaluation of Aquarius Level 2 Along-Track SSS

3.1. Comparison With In Situ Salinity Measurements

Figure 2 compares the Aquarius SSS and Argo salinity for (a) the V3.0, (b) the CAP V3.0, and (c) the RSS algorithms. The numbers of the collocated data are different (162,566 for V3.0 and 166,660 for CAP) despite the same duration because the numbers of missing values are different between them. In general, the Aquarius

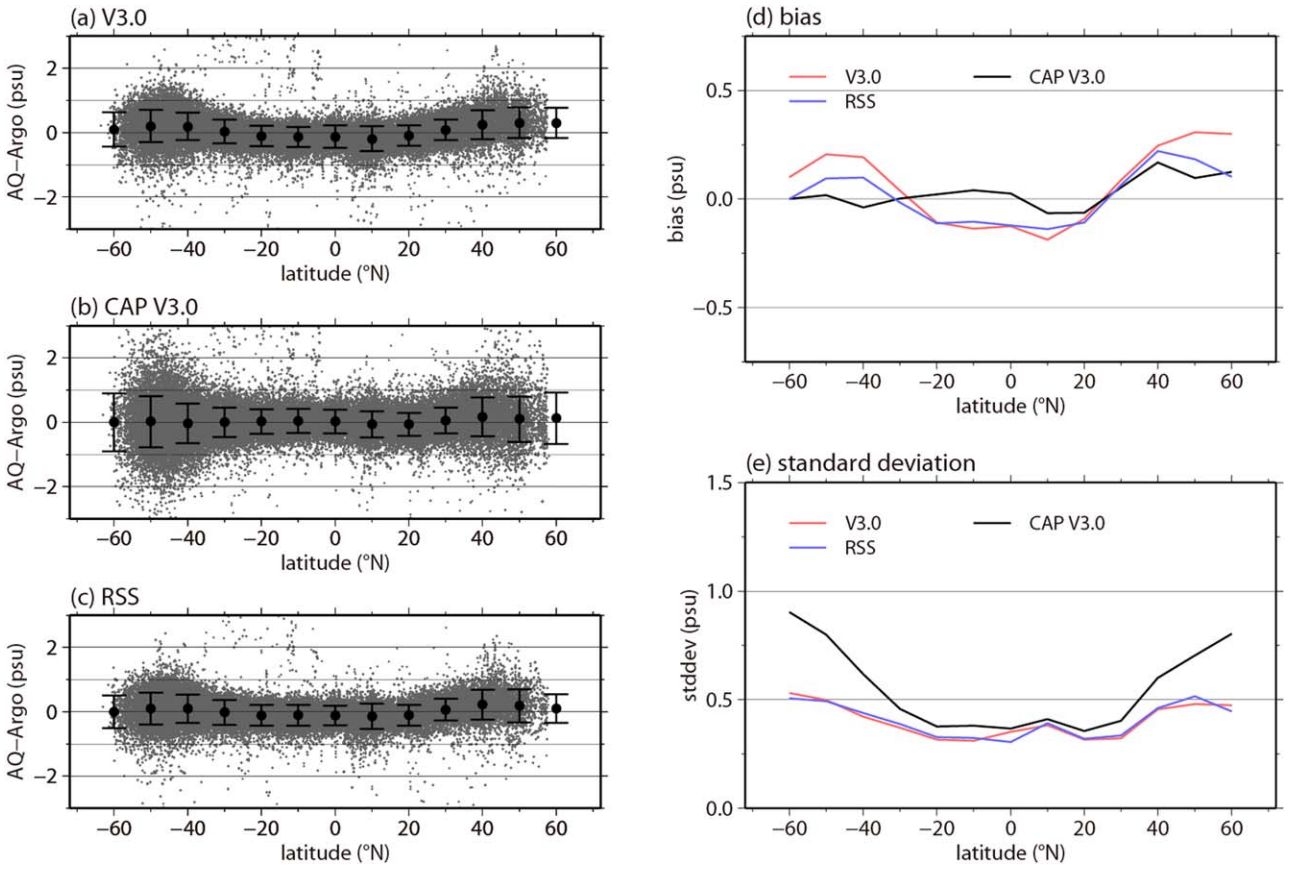

Figure 6. Dependence of salinity residual (Aquarius SSS minus Argo salinity) on latitude for (a) V3.0, (b) CAP V3.0, and (c) RSS beam 1 products, superposed with the average (black dot) and standard deviation (vertical bar) calculated in 10° bins. (d) Average and (e) standard deviation computed using V3.0 (red line), CAP V3.0 (black line), and RSS products (blue line).

SSS agrees well with the Argo salinity for all three products. Although the overall characteristics of the Aquarius SSS in V3.0 and RSS match-up distributions are nearly identical, the CAP SSS features differ slightly, with the CAP SSS deviating largely from the Argo data for Argo values of approximately 34 psu (Figure 2b). The bias, defined by Aquarius SSS minus Argo salinity, is smaller than ± 0.02 psu for all the three data products. The rms differences range from 0.41 to 0.52 psu, with the CAP product having the largest rms difference. Similar results were obtained for beams 2 and 3 (not shown).

Figure 3 compares the three Aquarius SSS data sets with in situ salinity observations from moored buoys. Again, Aquarius SSS retrievals for all three products agree well with the buoy salinity observations, with no significant discernible differences amongst the products. The values of the rms differences shown in Figure 3 are smaller than those for the Argo data comparison (Figure 2) because, as to be discussed in section 3.3, the moored buoys are located in tropical regions.

3.2. Ascending Versus Descending Difference

Lagerloef et al. [2013] reports that in the previous Aquarius SSS product (version 2.0) a systematic bias exists between Aquarius SSS data observed along ascending (south-to-north portion of orbit) paths and descending (north-to-south portion of orbit) paths (A/D difference). The A/D difference and its seasonal oscillation have been conjectured to be caused by inaccurate corrections for the reflection of galactic radiation.

Figure 4 shows the examples of the monthly averaged ascending-descending difference for (a) the V3.0, (b) the CAP V3.0, and (c) the RSS beam 1 products. This A/D difference continues to be detected even in the relatively new Aquarius products (Figure 4). In the Southern Ocean, the seasonal oscillation of the A/D difference has its positive phase in March and its negative phase in September. This A/D difference was also detected in the beams 2 and 3 products (not shown). The A/D differences in the map were zonally averaged

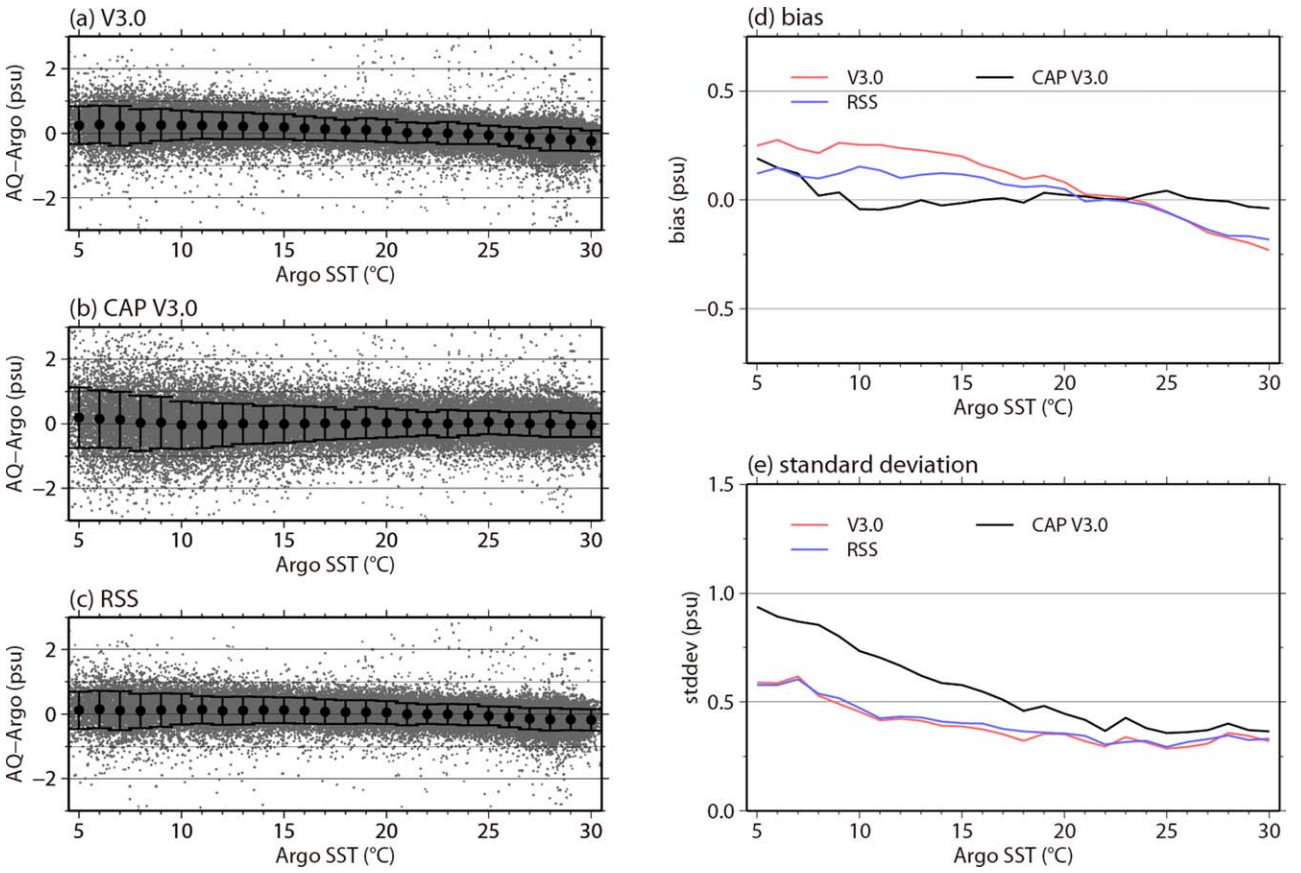

Figure 7. Same as Figure 6, except for dependence of the salinity residual (Aquarius SSS minus Argo salinity) for beam 1 on Argo sea-surface temperature (SST).

to make the latitude-time diagram of the difference in Figure 5. While the RSS product has large amplitudes of A/D differences in the Southern Ocean (Figure 5c), the amplitudes are considerably reduced in the V3.0 and CAP products (Figures 5a and 5b). In the Southern Ocean, the seasonality of the A/D difference in the CAP data is less clear than in the V3.0 data, suggesting another source of bias other than the galactic signal. In the higher latitudes of the North Hemisphere, a thin zonal negative difference band is found at 50°N, which is common to all three data sets. However, this feature may not be a robust signal because the numbers of data points at this latitude were small due to intense RFI, low SST, and high winds.

3.3. Residual Analyses

Figure 6 shows the dependence of the salinity residual (Aquarius SSS minus Argo salinity) on latitude calculated using (a) the V3.0, (b) the CAP V3.0, and (c) the RSS products for beam 1. The average and standard deviation of the salinity residual are computed in bins of 10° latitude and shown, respectively, by black dots and vertical bars in the left plots of Figure 6. The same bias and standard deviation are also plotted as thick lines in the top-right and bottom-right plots. For the V3.0 and RSS products, the bias is negative at low to middle latitudes (30°S–30°N) and positive at high latitudes, showing a symmetrical pattern of bias between the Northern and Southern Hemispheres. This equatorically symmetric pattern of the bias is not found for the CAP product. In general, the amplitude of the bias in the CAP product is smaller than the V3.0 and RSS products. Values of the standard deviation for all three products are less than 0.5 psu at 30°S–30°N and increase with latitude. The CAP V3.0 shows larger standard deviation than the V3.0 and RSS.

Figure 7 shows the dependence of the salinity residual on Argo sea-surface temperature (SST). The SSS biases in the V3.0 and RSS products are characterized by a notable trend that shifts from positive bias at low SST values to negative bias with increasing SST. The SSS bias increases to −0.20 psu for high SST conditions (>25°C). This result corresponds with the negative bias at low latitudes seen in Figure 6. The formation of salinity stratification in the near-surface layer caused by precipitation in tropical regions is one possible

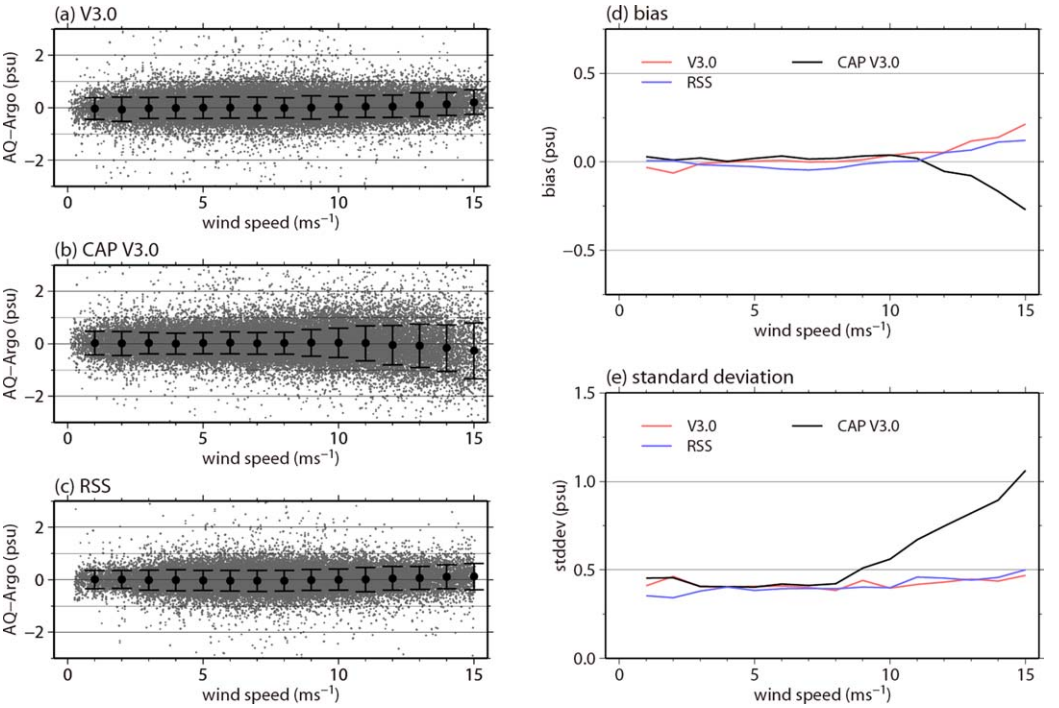

Figure 8. Same as Figure 6, except for dependence of the salinity residual (Aquarius SSS minus Argo salinity) for beam 1 on scatterometer wind speed.

reason for the negative bias. The CAP product also shows a negative bias trend under high SST conditions although the amplitude is quite small. The standard deviation of the salinity residual clearly depends on SST for all the three products. The value is relatively small (<0.5 psu) under high SST conditions (>20°C) and relatively large (>0.5 psu) under low SST conditions (<10°C).

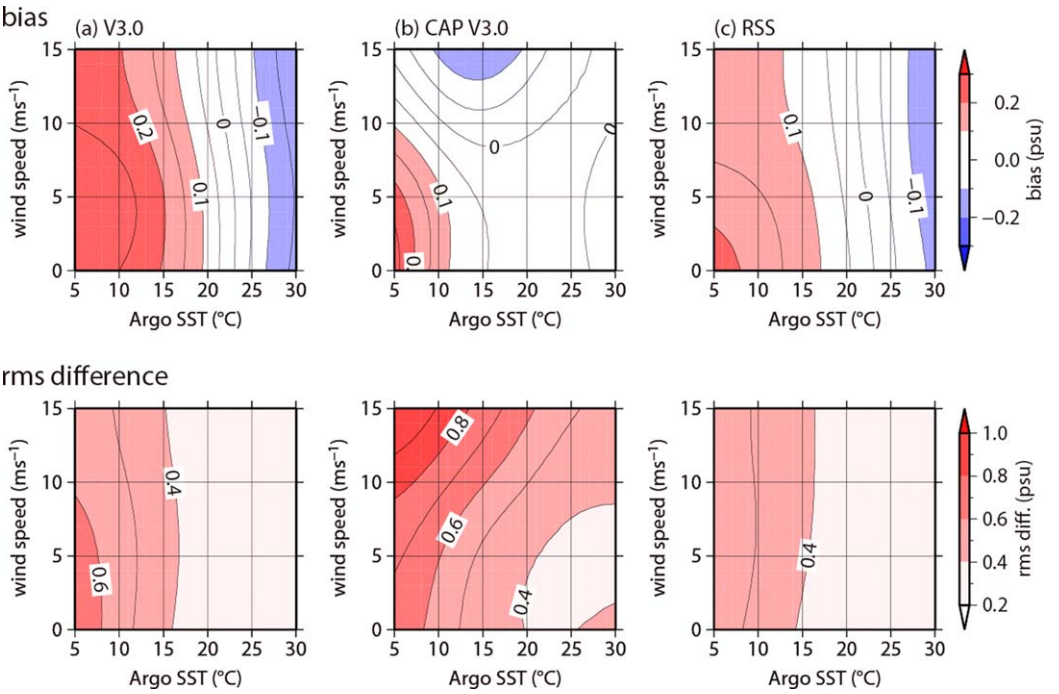

Figure 9. (top) Bias and (bottom) rms difference calculated from salinity residual (Aquarius SSS minus Argo salinity) expressed as a function of Argo sea-surface temperature (SST) and scatterometer wind speed determined using (a) V3.0, (b) CAP V3.0, and (c) RSS products for beam 1. The bias and rms difference are calculated in bins of 1°C and 1 m s^{-1} and then smoothed by a Gaussian filter with e-folding scales of 5°C and 5 m s^{-1}.

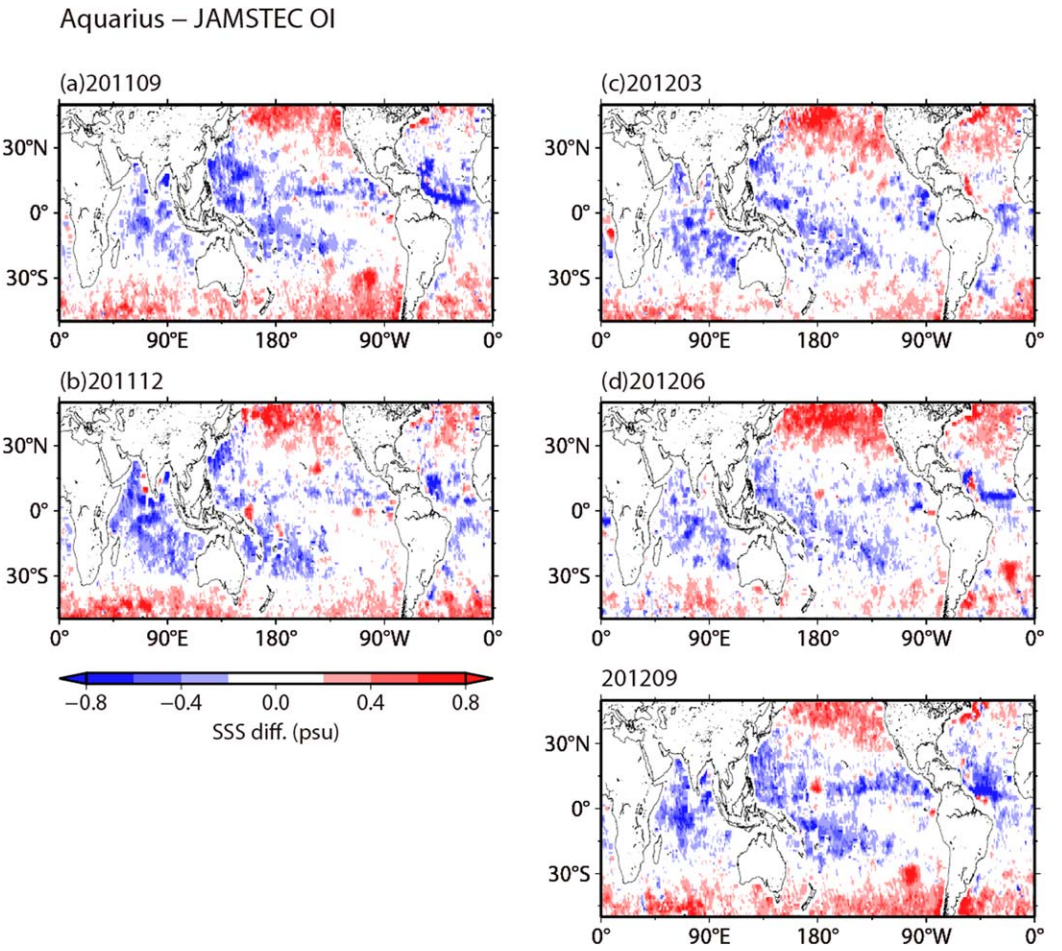

Figure 10. Monthly averaged sea-surface salinity (SSS) difference between Level 3 Aquarius V3.0 and JAMSTEC OI from September 2011 to September 2012 at 3-month intervals.

Figure 8 shows the dependence of the salinity residual on wind speed, as measured by the Aquarius scatterometer. The salinity bias is no more than ±0.1 psu under low and middle wind conditions (<11 m s^{-1}). Under high wind conditions, large SSS bias is found for all the products (+0.1 to +0.2 psu for the V3.0 and RSS products and −0.3 to −0.2 psu for the CAP product at 15 m s^{-1}). The standard deviation of the salinity residual is small (<0.5 psu) under low wind speed conditions (<7 m s^{-1}) and it increases with wind speed, especially for the CAP product, which is significantly larger under strong wind conditions (>10 m s^{-1}).

As shown in Figures 6–8, the salinity residual exhibits correlations with latitude, SST, and wind speed. Similar results were obtained for beams 2 and 3 (not shown). However, in the global statistics, these three parameters are not independent of each other. Low SST and high wind speed are mainly observed at higher latitudes. At higher latitudes, the A/D difference discussed in section 3.2 may also contribute to the salinity residual.

Figure 9 shows the bias (top) and rms difference (bottom) of the salinity residual expressed as a function of Argo SST and scatterometer wind speed for the three Aquarius products (beam 1). The bias and rms difference are calculated in bins of 1°C and 1 m s^{-1} and then smoothed by a Gaussian filter with e-folding scales of 5°C and 5 m s^{-1}. The bias in the CAP product (Figure 9b) is smaller than that in the V3.0 and RSS products. The bias in the CAP shows large negative bias for 9–19°C, which has maximum amplitude under strong wind conditions. In the V3.0 (Figure 9a) and the RSS (Figure 9c), amplitudes of the bias increase when SST decreases for a constant wind speed. The rms difference in the CAP is largest under low SST and high wind speed conditions (<10°C and >10 m s^{-1}), which corresponds with the higher variability of the SSS residual for the higher latitude areas (Figure 6). The amount of microwave energy emitted from the sea surface is less sensitive to SSS under low SST conditions [*Swift and McIntosh*, 1983], and the sea-surface roughness correction under high wind conditions could be less accurate, possibly contributing to the larger rms differences under low SST and high wind speed

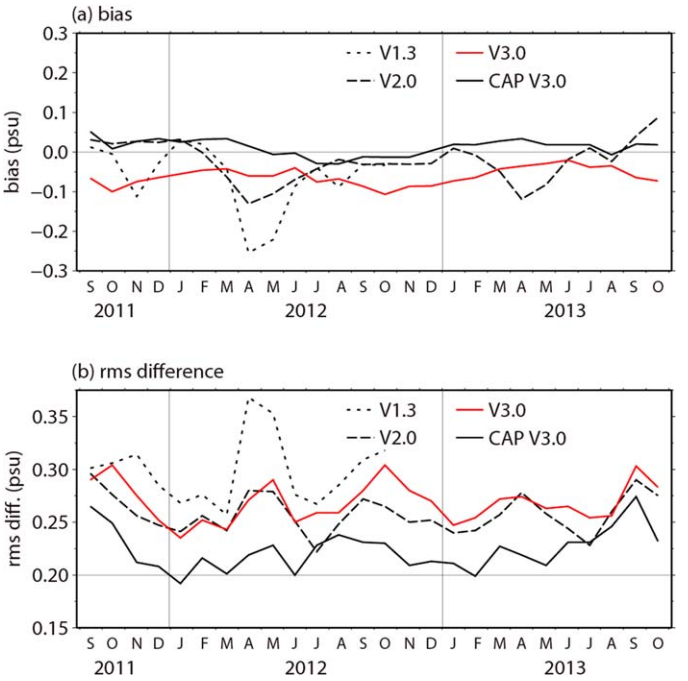

Figure 11. Time series of (a) bias and (b) rms difference calculated from salinity residuals (Aquarius SSS minus JAMSTEC OI salinity) using Level 3 Aquarius V1.3 (dotted line), V2.0 (dashed line), V3.0 (solid red line), and CAP V3.0 (solid black line) data from the area between 40°S and 40°N.

conditions at higher latitudes. In contrast, for the V3.0 and RSS products, the sensitivity of the rms differences to wind speed is weak, probably due to the algorithm refinements for the sea-surface roughness correction.

4. Evaluation of Aquarius Level 3 Monthly Averaged SSS

Figure 10 shows comparisons of monthly averaged Aquarius Level 3 SSS (V3.0) with outputs from the JAMSTEC OI system. The salinity residual is computed by subtracting the salinity in the JAMSTEC OI from the Aquarius SSS. Negative bias is discernible in tropical regions of the Pacific, Atlantic, and Indian Oceans. They are collocated with areas characterized by heavy rainfall, particularly in the Intertropical Convergence Zone (ITCZ) in each of the ocean basins and the South Pacific Convergence Zone (SPCZ), consistent with the tropical negative bias shown in Figure 6d. Large negative biases detected in the mid-latitude Asian Pacific are likely caused by radio frequency interference from the adjacent land area [*Lagerloef et al.*, 2013]. The negative bias seems to extend well beyond the typical RFI contamination region, particularly in September. Seasonal variation of precipitation distribution may also contribute to the seasonality of the negative bias in this region.

Figure 11 shows the time series of (a) bias and (b) rms difference of the salinity residual (Aquarius SSS minus JAMSTEC OI salinity) calculated over the global oceans (40°S–40°N). The average biases (rms differences) for the V1.3, V2.0, V3.0, and CAP V3.0 products are −0.06, −0.02, −0.06, and +0.01 psu (0.30, 0.26, 0.27, and 0.22 psu), respectively. As shown in Figure 11a, the early version of the Aquarius SSS, V1.3, exhibits amplitude variation in the bias that oscillates with a cycle of several months. The V1.3 and V2.0 exhibit negative bias peaks in April. The amplitude of the peak has been reduced in V3.0. Except for the bias peaks in April, V2.0 seems to generally perform better than V3.0. In the CAP V3.0, the amplitudes of the biases are further reduced. The rms difference in the Aquarius product is reduced from 0.30 psu (V1.3) to 0.27 psu (V3.0) by the algorithm refinements. The rms difference found in the CAP V3.0 product is further reduced to an average of 0.22 psu.

Figures 12 and 13 are the same as Figures 10 and 11, except the differences are with respect to outputs from MOVE/MRI.COM. The negative biases detected in the tropical regions and radio interference areas shown in Figure 10 also appear in Figure 12. In Figure 13, the average of the monthly biases (rms differences) shown for V1.3, V2.0, V3.0, and CAP V3.0 are −0.03, +0.00, −0.04, and +0.04 psu (0.28, 0.23, 0.24, and 0.20 psu), respectively. The rms difference in the CAP product is much smaller compared to the other products. Statistical features obtained from the comparison with the MOVE/MRI.COM outputs are essentially the same as those obtained by comparison with the JAMSTEC OI data, although the period of MOVE/MRI.COM data is shorter than that of JAMSTEC OI data.

It should be noted that the CAP data had the larger rms difference for Level 2 data (Figure 9), yet the smaller for the Level 3 products (Figures 11 and 13). Aside from the larger Level 2 uncertainty of individual retrievals, the bias in the CAP Level 2 product was smaller and temporally and spatially more stable. For the Level 3 product, uncertainty of the bias more directly influences the Level 3 differences with the JAMSTEC OI and

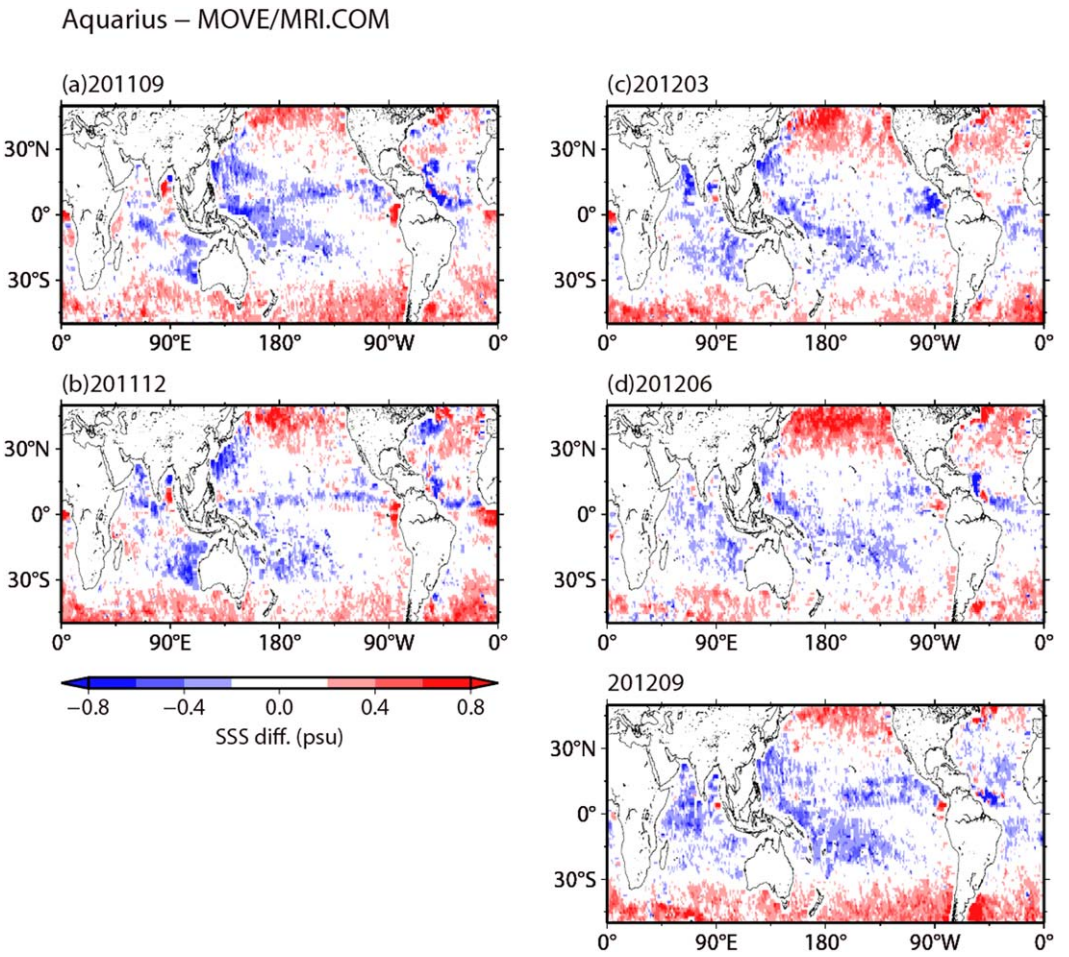

Figure 12. Monthly averaged sea-surface salinity (SSS) difference between Level 3 Aquarius V3.0 and MOVE/MRI.COM from September 2011 to September 2012 at 3-month intervals.

MOVE/MRI.COM data; therefore, the larger Level 2 rms difference and smaller Level 3 rms difference in the CAP V3.0 product are not considered to be inconsistent.

5. Summary

The SSS observed by Aquarius was validated by various sources of ocean surface salinity observations. The Level 2 Aquarius SSS data, produced by various salinity retrieval algorithms (V3.0, CAP V3.0, and RSS), were compared with in situ near-surface salinities obtained from global observations from Argo floats and moored buoys. The Aquarius SSS was collocated with the in situ salinity with spatial and temporal separations of $<$200 km and 12 h, respectively. In general, the SSS observed by Aquarius agrees well with the Argo and buoy measurements. The rms differences referenced to the Argo observations were 0.41–0.52 psu. In comparison with the moored buoy observations, the rms differences were 0.35–0.39 psu.

The SSS difference between the ascending and descending paths is discernible in all of the Aquarius products. This A/D difference exhibits seasonal oscillation with a large amplitude in the Southern Ocean. The amplitude of the A/D difference in the V3.0 and CAP products is reduced with respects to that of the RSS product. The seasonality of the A/D difference for the CAP product is not well defined. The standard deviations of the salinity residuals are large under low SST and high wind speed conditions, which is attributed to the low sensitivity of microwave emissivity to SSS at low SST and probable errors in the sea-surface roughness correction.

The Level 3 Aquarius monthly averaged SSS fields retrieved by the V3.0 and the CAP 3.0 were compared with outputs from the JAMSTEC ocean data OI and the MOVE/MRI.COM ocean data assimilation system.

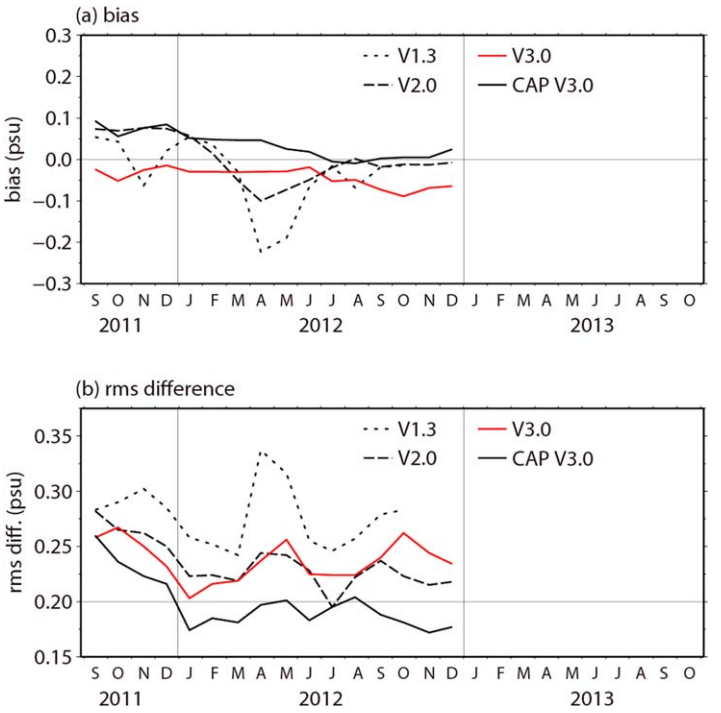

Figure 13. Time series of (a) bias and (b) rms difference calculated from salinity residuals (Aquarius SSS minus MOVE/MRI.COM salinity) using Level 3 Aquarius V1.3 (dotted line), V2.0 (dashed line), V3.0 (solid red line), and CAP V3.0 (solid black line) data from the area between 40°S and 40°N.

Negative biases, attributed to near-surface salinity stratification caused by precipitation in the ITCZ and SPCZ, were detected in tropical regions. Negative biases, likely due to radio frequency interference from adjacent land area, were also detected in the Asian Pacific. The rms difference of the salinity residual, with respect to the JAMSTEC OI, for 40°S–40°N was 0.27 psu for the V3.0, while, for the CAP V3.0, the average rms difference, was 0.22 psu, which is closer to the Aquarius mission goal of 0.2 psu.

In the Level 2 along-track SSS, the V3.0 and RSS products, with respect to in situ measurements, had smaller rms differences than the CAP product. In contrast, the SSS bias in the CAP product was small compared to the other products. The V3.0 and RSS products use SSS outputs from HYCOM to correct various SSS biases, while an external source of the SSS is not used in deriving the CAP product. The results from the V3.0 and RSS products were mostly the same except for the A/D difference, which was notably larger in the RSS product. For the Level 3 monthly gridded SSS products, the CAP product, with respect to the JAMSTEC OI and MOVE/MRI.COM, has smaller bias and rms difference than V3.0.

Acknowledgments

The authors thank the editor (Des Barton), an associated editor, and two anonymous reviewers who provided valuable comments to improve this paper. Financial support was provided by the Japan Society for the Promotion of Science (JSPS KAKENHI grant 23310001 and 22221001) and the Japan Aerospace Exploration Agency (JAXA). The authors are deeply grateful to Simon Yueh for providing the CAP product and for offering many valuable suggestions to improve this paper. They also thank Thomas Meissner for providing the SSS product made at RSS. The authors offer special thanks to Gary Lagerloef and Sandra Torrusio for providing them with the opportunity to join the Aquarius mission. The Aquarius V1.3, V2.0, V3.0, and CAP V3.0 products are available at the NASA/JPL PO.DAAC (http://podaac.jpl.nasa.gov/), and the RSS product is downloaded from the Remote Sensing Systems website (http://www.remss.com/). Data access to RSS product requires user registration. Please contact to the data producers (Thomas Meissner). Argo data are obtained from the Global Data Assembly Center through the US Global Ocean Data Assimilation Experiment (USGODAE) ftp server (http://www.usgodae.org/argo/argo.html) and offshore moored buoy data are from the NOAA Pacific Marine Environmental Laboratory (PMEL) website (http://www.pmel.noaa.gov/). The salinity data from the MOAA/GPV are available at the JAMSTEC website (http://www.jamstec.go.jp/), and those from the MOVE/MRI.COM are obtained from the data producer, MRI/JMA (http://www.mri-jma.go.jp/).

References

Bourlès, B., et al. (2008), The PIRATA program: History, accomplishments, and future directions, *Bull. Am. Meteorol. Soc.*, *89*, 1111–1125.

Chassignet, E. P., et al. (2009), U.S. GODAE: Global ocean prediction with the HYbrid Coordinate Ocean Model (HYCOM), *Oceanography*, *22*(2), 48–59.

Hosoda, S., T. Ohira, and T. Nakamura (2008), A monthly mean dataset of global oceanic temperature and salinity derived from Argo float observations, *JAMSTEC Rep. Res. Dev.*, *8*, 47–59. [Available at http://www.argo.ucsd.edu/Hosoda_etal_MOAA_GPV.pdf.]

Kuroda, Y. (2002), TRITON: Present status and future plan, *TOCS Rep. 5*, pp. 77, Jpn. Mar. Sci. and Technol. Cent., JAMSTEC, Japan.

Lagerloef, G., et al. (2008), The Aquarius/SAC-D Mission: Designed to meet the salinity remote-sensing challenge, *Oceanography*, *21*(1), 68–81.

Lagerloef, G., et al. (2013), *Aquarius Salinity Validation Analysis, Data Version 2.0, Aquarius Project Document AQ-014-PS-0016*, pp. 36. [Available at http://aquarius.umaine.edu/docs/AQ-014-PS-0016_AquariusSalinityDataValidationAnalysis_DatasetVersion2.0.pdf.]

LeVine, D. M., G. S. E. Lagerloef, and S. E. Torrusio (2010), Aquarius and remote sensing of sea surface salinity from space, *Proc. IEEE*, *98*(5), 688–703.

McPhaden, M. J., et al. (1998), The Tropical Ocean-Global Atmosphere observing system: A decade of progress, *J. Geophys. Res.*, *103*(C7), 14,169–14,240.

McPhaden, M. J., G. Meyers, K. Ando, Y. Masumoto, V. S. N. Murty, M. Ravichandran, F. Syamsudin, J. Vialard, L. Yu, and W. Yu (2009), RAMA: The Research Moored Array for African-Asian-Australian Monsoon Analysis and Prediction, *Bull. Am. Meteorol. Soc.*, *90*, 459–480.

Meissner, T. (2013), *Aquarius L2 RSS Testbed: Data Set Description and User Manual*, pp. 14. [Available at http://oceania.research.um.edu.mt/cms/smosmode/downloads/RSS_testbed_user_manual.pdf.]

NASA JPL PO.DAAC (2014), *Aquarius User Guide, Aquarius Dataset Version 3.0 (Guide Version 6.0)*, JPL-D70012 AQ-010-UG-008, pp. 86. [Available at http://aquarius.umaine.edu/docs/AquariusUserGuide_DatasetV3.0.pdf.]

Patt, F. S. (2014), *Aquarius Level-2 Data Product, Aquarius Project Document AQ-014-PS-0018 Version 3.0*, pp. 23. [Available at ftp://podaac-ftp.jpl.nasa.gov/allData/aquarius/docs/v3/AQ-014-PS-0018_AquariusLevel2specification_DatasetVersion3.0.pdf.]

Swift, C. T., and R. E. McIntosh (1983), Considerations for microwave remote sensing of ocean-surface salinity, *IEEE Trans. Geosci. Remote Sens.*, *21*(4), 480–491.

Usui, N., S. Ishizaki, Y. Fujii, H. Tsujino, T. Yasuda, and M. Kamachi (2006), Meteorological Research Institute multivariate ocean variational estimation (MOVE) system: Some early results, *Adv. Space Res.*, *37*, 806–822.

Wentz, F. J., and D. M. LeVine (2012), Aquarius salinity retrieval algorithm version 2: Algorithm theoretical basis document, *RSS Tech. Rep. 082912*, pp. 45. [Available at ftp://podaac-ftp.jpl.nasa.gov/allData/aquarius/docs/v2/AQ-014-PS-0017_AquariusATBD_Level2.pdf.]

Yueh, S., and J. Chaubell (2012), Sea surface salinity and wind retrieval using combined passive and active L-band microwave observations, *IEEE Trans. Geosci. Remote Sens.*, *50*(4), 1022–1032.